



# Shear Behavior of Reinforced Concrete Shallow Beams with Lightweight Infill

## (سلوك القص للكمرات التي تحوى بلوكات من الطوب الخفيف)

Ahmed M. Tahwia, Mohamed E. El-Zoughiby and Mohammed H. Hassan

### KEYWORDS:

*Lightweight infill material, In filled beams, Failure load, shear load, nonlinear finite element analysis*

*المخلص العربي - هذا البحث يلقى الضوء على تأثير احلال جزء من قطاع الكمرة المسلحة في منطقة الشد بمواد خفيفة الوزن لانقاص وزن الكمرة. و عليه تم دراسة تأثير الاستبدال على عدد ثلاثة نماذج، النموذج الأول (BS01) كمرة مصمته بدون احلال (مرجعية) و النموذج الثاني (BS02) كمرة تم احلال جزء منها باستخدام عدد 4 بلوكات من الطوب الخفيف مع ترك أعصاب بعرض 100 مم بين البلوكات واخيرا نموذج (BS03) كمرة تم احلال جزء منها باستخدام عدد 8 بلوكات من الطوب الخفيف مع ترك أعصاب بعرض 40 مم بين البلوكات. و قد تم اختبار الكمرات في المعمل حتى حمل الانهيار. و تم عمل نمذجة للكمرات المسلحة السابقة باستخدام برنامج (ANSYS 15.0). و تمت المقارنة بين نتائج الاختبارات المعملية و نتائج التحليل العددي باستخدام البرنامج و تبين أنه نتيجة لصغر القطاع الخرساني للكمرة بسبب احلال جزء من القطاع الخرساني ببلوكات من الطوب الخفيف فقد تغير شكل الكسر في هذه الكمرات.*

**Abstract** - This paper presents the effect on the shear behavior of reinforced concrete shallow beams due to infilling by using the Autoclaved Aerated Concrete (AAC) as a lightweight material to decrease the weight of the beams. Three reinforced concrete beams were fabricated in the lab to study the effect of infilling the beams with AAC blocks. The first beam is a solid or reference beam, SB01. The second beam was in filled by four AAC blocks having 100mm thick ribs, SB02. The last beam was also in filled but with eight AAC blocks having 40mm thick ribs, SB03. Based on the experimental shear test of the three beams, the test results were recorded and investigated. Additionally, 3-D, a nonlinear finite element analysis to simulate the behavior of the three beams by ANSYS 15.0-package was carried out. The experimental results of the beams were discussed and compared with the numerical outputs. It's found that decreasing the concrete section due to infilling changes the type of failure mode of the tested beams compared to the solid one.

### I. INTRODUCTION

Reducing the self-weight of the concrete parts is the subject of many studies. It becomes important due to the wide use of reinforced concrete elements in many constructions in the world. The decreasing of structure self-weight saves the used materials quantity, manpower, structure cost, the construction equipment, and reduces the foundation cost. There are many technologies to decrease the concrete self-weight, such as using lightweight aggregate with big voids. This, as in precast units, reduces the projects process and saves the cost of the material and the equipment [1]. Another technology was used to reduce the self-weight of reinforced concrete elements were the concrete between the top and bottom steel layer in slab was replaced by spherical made from high density polypropylene (Bubble-Deck) [2]. Others were infilling lightweight material in beams in the cracking zone under the natural axis. This helps to reduce the beam's self-weight without reducing its strength [3]. The Autoclaved Aerated Concrete AAC blocks were used as lightweight infill materials in reinforced concrete beams and slabs [4]. To reduce the self-weight without sacrificing the structural capacity, Yardim, had infilled the semi precast panels by using AAC blocks [5].

Received: 21 February, 2018 - Revised: 12 April, 2018 - Accepted: 24 April, 2018

Ahmed M. Tahwia, Prof., Structural Engineering Dept., Faculty of Engineering, Mansoura University, Egypt.

Mohamed E. El-Zoughiby, Associate Prof., Structural Engineering Dept., Faculty of Engineering, Mansoura University, Egypt.

Mohammed H. Hassan, Research scholar, Structural Engineering Dept., Faculty of Engineering, Mansoura University, Egypt.

II. EXPERIMENTAL ANALYSIS

A. Materials:

1) Concrete

The Self-Compacting Concrete (SCC) was used in fabricating the in filled beams having narrow spaces (ribs) between AAC blocks and around the bars. Table 1 shows the by-weight components of SCC. The CEM I 42.5N produced by El-Suez Cement Company was the used cement. The used fine aggregate was from local natural sand composed mainly of siliceous materials with a specific gravity of 2.50 and a fineness modulus of 2.66. The coarse aggregate that was used is crushed dolomite with a specific a gravity of 2.71 and a maximum nominal size of 10 mm. The average concrete compressive strength was 36 MPa.

TABLE I  
THE SCC MIX PROPORTIONS (kg/m<sup>3</sup>)

Cement	CA <sup>a</sup>	FA <sup>b</sup>	Water	Superplasticizers
425	860	860	200	8.5

a= Course aggregate

b Fine aggregate

2) Autoclaved aerated concrete (AAC)

Autoclaved aerated concrete AAC is a kind of lightweight concrete made in blocks shape. It was produced by adding a predetermined amount of aluminum powder and other additives to slurry of ground high silica sand, cement or lime, and water [6]. The dimensions of the AAC blocks in this study were 100 mm × 200 mm × 600 mm with dry density of 600kg/m<sup>3</sup>. Four blocks 100 mm × 200 mm × 600 mm were used to infill beam BS02, Fig. 2. Whereas eight blocks 100 mm × 200 mm × 300 mm were used to infill beam BS03, Fig. 3. The average compressive strength of the AAC cubes (100 mm × 100 mm × 100 mm) was 4.0 MPa.

3) Reinforcing bars

Top and bottom longitudinal bars were provided. The bottom bars were 18 mm diameter and the top bars were 10mm diameter. Each beam had 16 stirrups with 8mm diameter as shown in Figs. 2 and 3. The yield strength of steel bars was 360 MPa for longitudinal bars and 240 MPa for stirrups.

B. Test Beams

Three beams were cast for shear test. Each beam has a rectangular cross section 200 mm by 350 mm, Fig. 1. The length was 3000 mm. The first beam SB01, a reference beam, was a solid beam without infill blocks. The second beam SB02 was in filled by AAC blocks (100 mm × 200 mm × 600 mm) and the width of ribs between blocks was 100mm, Fig. 2. The third beam SB03 was infilled by AAC blocks (100×200×300mm) and the width of ribs between the blocks was 40 mm, Fig. 3. The weight reduction due to the infill AAC blocks was about 17.5% of that of the solid beam.

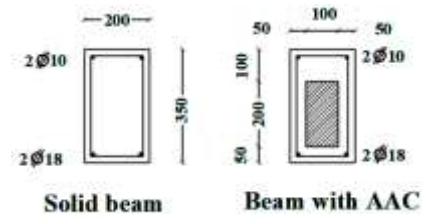


Fig. 1. Beams cross sections

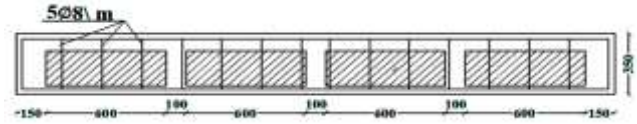


Fig. 2. Beam SB02 details.

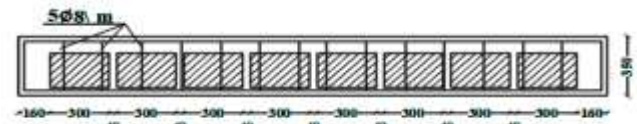


Fig. 3. Beam SB03 details.

C. Test set up

As shown in Figs. 4 and 5, the tested beams are supported on two steel rollers bearing near its ends and are loaded through similar steel bearings placed at two points at its top. This means a constant bending moment in its middle part between the load points. The clear span between the two supports is 2800 mm and the distance between the load points is 1600mm. For all tested beams, the shear span-to-depth ratio (a/d) was 1.91. Each beam was loaded up to failure. The vertical loading was gradually applied during the loading process, the mid-span displacements were measured, and all

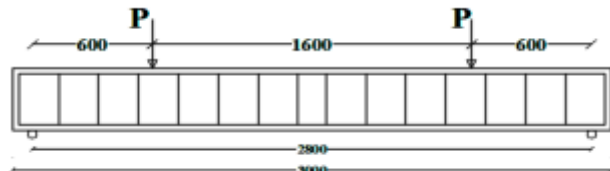


Fig. 4. Load and supports arrangement



Fig.5 Test set-up

formed cracks and the corresponding loads were redrawn with a marker pen. Just after failure, photos are taken to show the crack pattern and the mode of failure.

**D. Output results and discussion**

For the three tested beams, the flexural cracks were appeared in the beam central zone and the shear cracks were appeared in the zone between the load and the support at each beam end and, then, spread gradually towards the supports at early load stages. The failure load and the corresponding mid-span deflection for beam BS01 was 185 kN and 16.46 mm, for beam BS02 was 185 kN and 14.72 mm, and for beam BS03 was 180 kN and 15.80 mm, respectively, Table 2.

TABLE 2  
THE OUTPUT RESULTS

Beam	Weight (kN)	Failure Load (kN)	Mid-Span Deflection (mm)
BS01	525	185	16.46
BS02	434	185	14.72
BS03	434	180	15.80

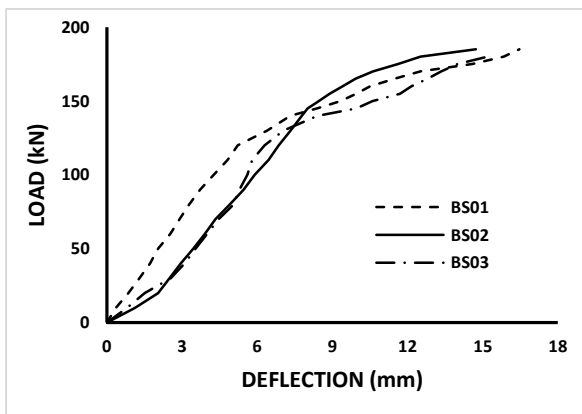


Fig. 6 Mid-span load-deflection curve

With reference to Fig. 6, the load-deflection curve at mid-span for all beams indicates almost the same tendency of deformations.

At early loading stages, the flexural cracks appeared in the central portion for all tested beams and, by loading, the shear cracks appeared near the supports, and the cracks spread gradually towards the supports. The number and widths of cracks were, then, increased in the portion between the two-point loads. Figs. 7 to 12 show the crack pattern and the main crack at failure for beams BS01, BS02, and BS03, respectively. For all tested beams, the mode of failure for beam BS01 was shear, but for beams BS02 and BS03 was diagonal tension failure.

The failure loads of the beams BS01 and BS02 are similar and were greater than that of the beam BS03 by about 3%. The beams, however have different failure modes. This could be due to decreasing the concrete section in the in filled beams

compared to the solid one. The vertical deformation was a maximum at the mid-span of the beams. The mid-span deflection for the in filled beams BS02 and BS03 was less than that of the solid beam BS01.



Fig. 7 Crack pattern of Beam BS01

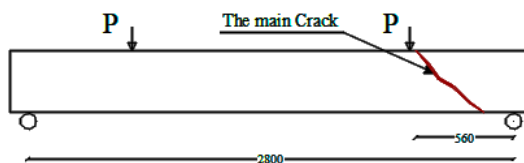


Fig. 8 Main crack at failure for BS01



Fig. 9 Crack pattern of Beam BS02

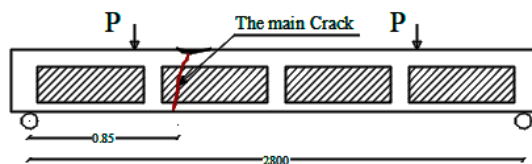


Fig. 10 Main crack at failure for BS02



Fig.11 Crack pattern of Beam BS03

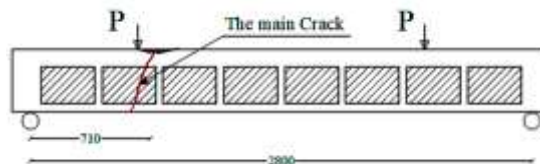


Fig 12 Main crack at failure for BS03

III. NUMERICAL ANALYSIS

To numerically investigate the shear behavior of the tested RC beams, a 3D nonlinear finite element analysis based on ANSYS 15.0- package have been carried-out. This helps to completely understand the shear behavior of the beams.

A. Modeling

The material of the model both concrete and rebar, the modeling of the beam's supports, the failure criteria, meshing, and bounding conditions are next discussed.

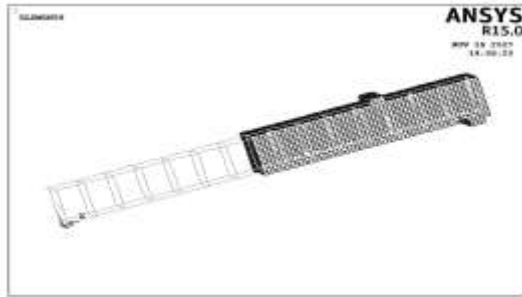


Fig.13 Control beam BS01

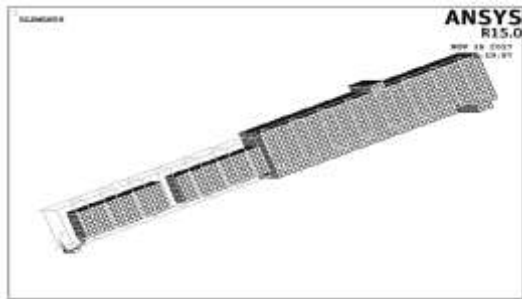


Fig. 14 In filled beam BS02

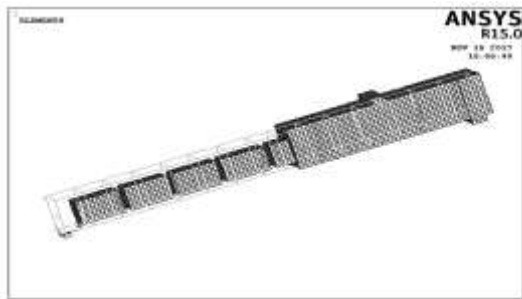


Fig.15 In filled beam BS03

1) Concrete

The Solid65 element was used to model the concrete and AAC blocks, the 3D modeling of solids with or without reinforcing bars. It is capable of cracking in tension and crushing in compression. The element is defined by eight nodes with three degrees of freedom at each in x, y, and z directions. The element stress directions are parallel to the element coordinate system. The concrete was defined as an isotropic hardening plastic material and the considered compressive uniaxial stress-strain formulas are shown in Figs. 16 and 17, respectively [6]. The material properties are shown in Table 3.

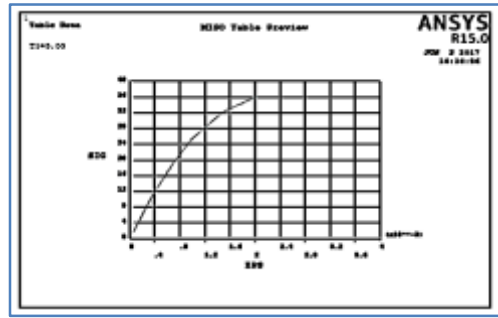


Fig. 16. The concrete stress-strain relationship

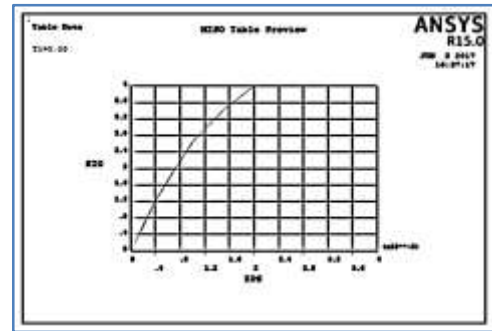


Fig.17 AAC stress-strain relationship

2) Rebar

The Link180 element was the appropriate element to simulate the steel reinforcing bars. It is a uniaxial tension-compression element with three translational degrees of freedom at each node in x, y, and z directions. Perfect bond between concrete and rebar can be assumed upon sharing the same nodes between the rebar and concrete elements. The idealized stress-strain curve in Fig.18 was used to define the steel elastic-plastic behavior. The rebar input material properties are shown in Table 3.

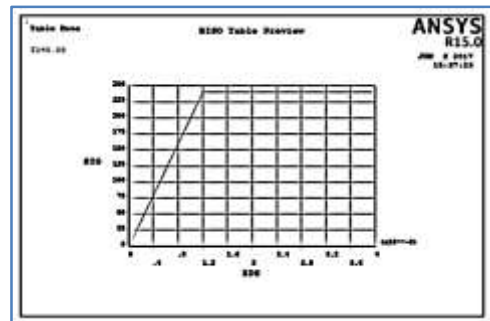


Fig. 18 Steel stress-strain relationship

3) End supports

The end supports plate for all considered beams should be rigid. The Solid45 element was the best to simulate end supports. It is used for the three-dimensional modeling of solid structures and is defined by eight nodes with three degrees of freedom in the x, y, and z directions. The material properties are as shown in Table 3

TABLE 3  
MATERIAL PROPERTIES

Element	Material	Material properties			
Solid65	Concrete	<b>Linear Isotropic</b>			
		EX	30000		
		PRXY	0.3		
		<b>Multilinear Isotropic</b>			
		Point	Strain	Stress	
		1	0.00036	10.8	
		2	0.0007	19.354	
		3	0.001	25.562	
		4	0.0015	32.36	
		5	0.0024	36	
		6	0.003	36	
		<b>Concrete Coefficients</b>			
		Open shear coff.	0.4		
		Closed shear coff.	0.85		
		Uniaxial tensile. str.	2.5		
	Uniaxial comp. str.	36.0			
	Tensile crack factor	0.6			
	AAC	<b>Linear Isotropic</b>			
		EX	3000		
		PRXY	0.2		
		<b>Multilinear Isotropic</b>			
Point		Strain	Stress		
1		0.0004	1.2		
2		0.0007	1.96		
3		0.001	2.63		
4		0.0015	3.41		
5		0.0027	4		
6		0.003	4		
<b>Concrete Coefficients</b>					
Open shear coff.		0.35			
Closed shear coff.		0.85			
Uniaxial tensile. str.		0.5			
Uniaxial comp. str.		4.0			
Tensile crack factor	0.6				
Link180	Mild Steel	<b>Linear Isotropic</b>			
		EX	2 x 105		
		PRXY	0.3		
		<b>Bilinear Isotropic</b>			
		Yield stress	240		
	Tangent modulus	20			
	High Grade Steel	<b>Linear Isotropic</b>			
		EX	2 x 105		
		PRXY	0.3		
		<b>Bilinear Isotropic</b>			
Yield stress		360			
Tangent modulus	20				
Solid45	Steel plate	<b>Linear Isotropic</b>			
		EX	2 x 106		
		PRXY	0.3		

4) Failure criteria

Failure criteria are commonly used for determining the damage initiation in orthotropic materials. Based on various assumptions on the material damage mechanism, failure criteria are usually formulated with functions of element solution (stresses or strains) and material strength limits. The cracking and crushing of failure mode are depended on the uniaxial tensile and compressive strength values, and define the failure surface for concrete. William and Warnke proposed a formula to calculate the failure of the concrete by the multi-axial stress state. In a concrete element, cracking occurs when the principal tensile stress in any direction lies outside the failure surface. When the concrete had cracking, the elastic modulus of the concrete element is set to zero in the direction parallel to the principal tensile stress direction. Crushing happened when the principal stresses are compressive and straight to outside the failure surface; subsequently, the elastic modulus is set to zero in all directions [7].

5) Meshing and boundary conditions

The finite element models in the numerical program were input with overall dimensions of 200x350x3000mm. The beams were, then, divided by elements spaced at 25mm. The number of elements for the considered beams is as shown in Table 4.

TABLE 4  
NUMBER OF ELEMENTS IN EACH BEAM

Element	Material	Beams		
		BS01	BS02	BS03
Solid 65	concrete	13440	10368	11296
	ACC	-	3072	3264
Link180	Steel bar	1056	1056	1096
Solid 45	End plate	256	256	256
<b>Total</b>		14860	14752	14752

B. Finite element analysis results

The three reinforced concrete tested beams (solid beam BS01, in filled beam BS02 using AAC blocks with 100mm ribs, and in filled beam BS03 using AAC blocks with 40mm ribs) were modeled and analyzed based on ANSYS-15 package. The beams were gradually loaded until failure. The obtained results, such as the failure load, the mid-span deflection, the first cracking load, and the crack pattern were compared with the experimental results.

TABLE 5  
THE FAILURE LOAD AND THE MID-SPAN DEFLECTION

Beam	BS01	BS02	BS03
<b>Failure Load, (kN)</b>	190.1	189.2	192.8
<b>First Cracking Load, (kN)</b>	80.47	69.94	66.41
<b>Mid-Span Deflection, (mm)</b>	12.75	12.64	14.44

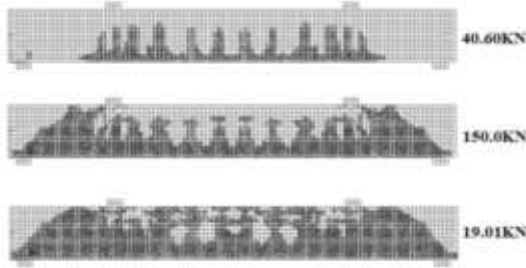


Fig. 19 The beam BS01 crack patterns

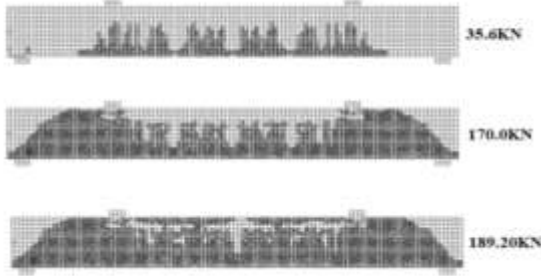


Fig. 20 The beam BS02 crack patterns

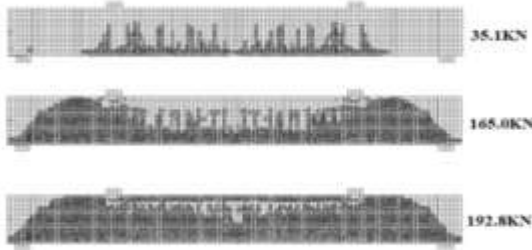


Fig. 21 The beam BS03 crack patterns

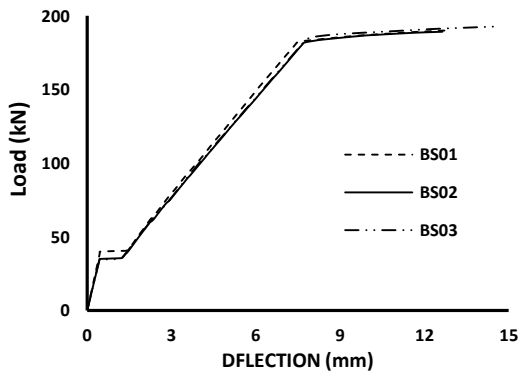


Fig. 22 The load-deflection curve

AAC blocks and the width of the concrete ribs between the ACC blocks on the shear behavior of the considered reinforced concrete beams.

TABLE 6  
EXPERIMENTAL VS. THE NUMERICAL FAILURE LOAD AND THE MID-SPAN DEFLECTION FOR BEAM BS01

Beam BS01	Failure Load, (kN)	Mid-Span Deflection, (mm)
Experimental	185	16.46
Numerical	190.1	12.75

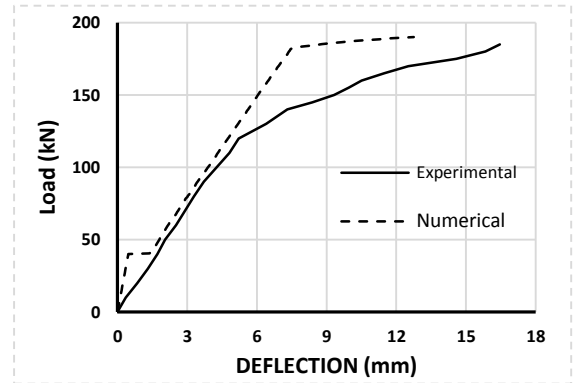


Fig. 23 Load-deflection curve for beam BS01

TABLE 7  
EXPERIMENTAL VS. THE NUMERICAL FAILURE LOAD AND THE MID-SPAN DEFLECTION FOR BEAM BS02

Beam BS02	Failure Load, (kN)	Mid-Span Deflection, (mm)
Experimental	185	14.72
Numerical	189.2	12.64

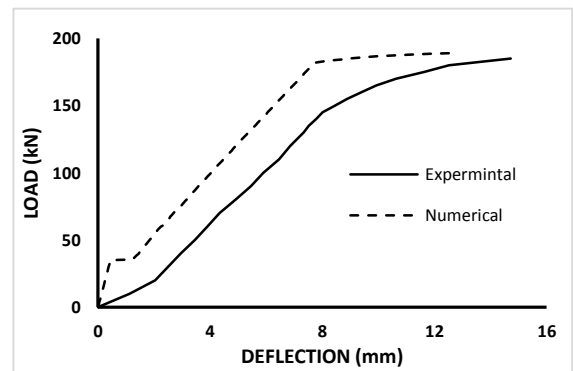


Fig. 24 Load-deflection curve for beam BS02

C. Numerical versus experimental results

The comparison between the numerical model output and the experimental results includes the failure load, the mid-span deflection, and the first cracking load. The comparison shows the effect of both of infilling reinforced concrete beams with

TABLE 8  
EXPERIMENTAL VS. THE NUMERICAL FAILURE LOAD AND THE MID-SPAN DEFLECTION FOR BEAM BS03

Beam BS03	Failure Load, (kN)	Mid-Span Deflection, (mm)
Experimental	180	15.8
Numerical	192.8	14.44

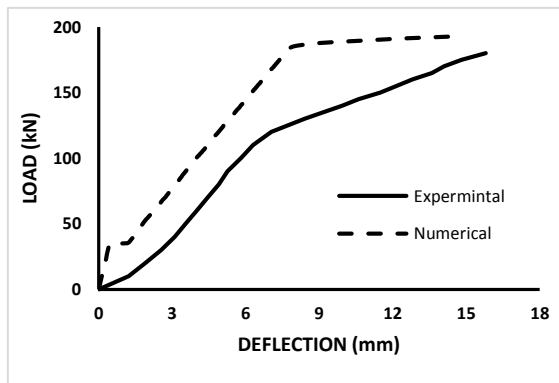


Fig. 25 The load-deflection curve for beam BS03

The variance between the numerical model and the experimental tests results was about 2.7% for beam BS01, 2.3% for beam BS02 and 7.2% for beam BS03. The crack patterns in Figs. 19 to 21 explain the beams crack pattern clearly presents this point. The failure load of the solid beam BS01 and the in filled beam BS02 was almost same and less than that of the in filled beam BS03 by about 1.8%. The mid-span deflection for of the solid beam BS01 and the infilled beam BS02 was almost the same and less than that of the infilled beam BS03 by about 13%.

#### D. Conclusions

Based on upon comparing the experimental test results and the numerical model outputs of the three considered beams under shear loads, the following conclusions can be drawn:

- Under the shear test, the failure mode of solid beam BS01 was a shear failure, but the infilled beams failure mode was a diagonal tension failure.

- The maximum deflection was in the mid-span for all tested beams.
- The failure load of the beams BS01 and BS02 were almost the same and greater than that of the beam BS03 by about 3%. But from the numerical analysis, it is found that the failure load of the solid beam BS01 and the infilled beam BS02 was almost same and less than that of the infilled beam BS03 by about 1.8%. The solid beams had failure model difference than the infilled beams. This could be due to decrease the concrete section in the infilled beams than the solid one. The infilled beam BS02 and BS03 have less self-weight than that of the solid beam BS01 by about 17.33%.
- From the experimental result found that the mid-span deflection for the infilled beams BS02 and BS03 was less than the solid beam BS01 by about 7% and 4% respectively. But for numerical analysis output the mid-span deflection for the beams BS01 and BS02 were same and less than that of the beam BS03 by about 12%.

- 

#### IV. REFERENCES

- [1] T. Y. Lo and H. Z. Cui, "Properties of green lightweight aggregate concrete," *International workshop on sustainable development and concrete technology*, Beijing, 2004, pp. 113-121.
- [2] S. Calin and C. Asavaoie, (2009), "Method for bubbled concrete slab with gaps," *Buletinul institutului politehnic din iasi*, 55(2), pp. 63-70.
- [3] P. Rakesh, D. S. Kumar and P. K. Kant, (2012), "Brick filled reinforced concrete composite beams," *Advanced engineering technology*, 3(2), pp. 124-126.
- [4] V. Vimonsatit, A. S. Wahyuni and H. Nikraz, (2012, July) "Reinforced concrete beams with lightweight infill," *Scientific research and essays*, 7(27), pp. 2370-2379.
- [5] Y. Yardim, A. M. Waleed, M. S. Jaafar and S. Laseima, (2013) "AAC-concrete light weight precast composite floor slab," *Construction and building materials*, (40), pp. 405-410.
- [6] D. Kachlakev, T. Miller and T. poitsuk, (2001), "Finite element modeling of concrete structures strengthened with FRP laminates," *Oregon department of transportation, research group*.
- [7] K. J. William and E. P. Warnke, (1974) "Constitutive model for the triaxial behaviour of concrete," *International association for bridge and structural engineering proceedings*, (19), pp. 1-30.
- [8] A. J. Hamad, (2014), "Materials, production, properties and application of aerated lightweight concrete: review," *International journal of materials science and engineering*, 2(2), pp. 152-157.